Surface spin-flop transition in a classical *XYZ* chain

1999 J. Phys. A: Math. Gen. 32 3275

(http://iopscience.iop.org/0305-4470/32/18/305)

J. Phys. A: Math. Gen. **32** (1999) 3275–3281. Printed in the UK PII: S0305-4470(99)99759-7

Surface spin–flop transition in a classical XYZ chain

J Karadamoglou and N Papanicolaou

Department of Physics, University of Crete and Research Center of Crete, Heraklion, Greece

Received 27 November 1998, in final form 1 February 1999

Abstract. A surface spin–flop transition has recently been observed in a multilayer Fe/Cr film (superlattice) that may be effectively described by a classical antiferromagnetic chain with a single-ion anisotropy. In this paper we explore such a transition in a classical spin chain with exchange anisotropy. Our theoretical results may suggest the occurrence of a similar phenomenon in quantum spin chains doped with nonmagnetic ions.

The recent experimental observation of a surface spin–flop (SSF) transition in an Fe/Cr superlattice [1–3] generally confirmed early theoretical ideas [4–6]. However, the finer details of the transition turned out to be rather intricate and are being clarified in a number of current theoretical investigations [7–13]. In these studies the superlattice is modelled by a classical spin chain with an isotropic antiferromagnetic exchange interaction and a single-ion anisotropy.

Here we propose to explore the possibility of a similar transition in the presence of an exchange anisotropy, in the context of spin systems described by the XYZ Hamiltonian [14]

$$W = \sum_{\ell=1}^{\Lambda-1} (J_1 S_\ell^x S_{\ell+1}^x + J_2 S_\ell^y S_{\ell+1}^y + J_3 S_\ell^z S_{\ell+1}^z) - H \sum_{\ell=1}^{\Lambda} S_\ell^z \tag{1}$$

defined on an open chain with Λ sites. In practice, spin chains of finite size can be produced through doping with nonmagnetic ions and various surface effects may then be investigated [15]. However, there seems to have been no experimental or theoretical attention to the possibility of a SSF transition, except for a peripheral comment made in [16]. We thus initiate a theoretical study of such a transition in the *classical XYZ* model, whose aim is twofold: first, to provide an alternative example that may indirectly illuminate some of the darker features of classical superlattices and secondly to set the stage for the study of similar effects in quantum spin chains which are, of course, more relevant for the description of crystalline magnets.

The class of Hamiltonians (1) will be restricted by the inequalities $|J_1| \leqslant J_2 < J_3$ which contain as a special case the antiferromagnetic XXZ or Heisenberg–Ising chains ($J_1 = J_2$). We shall only discuss the classical minimum (ground state) of (1) which turns out to be independent of the specific value of J_1 in the above parameter range. In other words, the minimum is achieved with a spin configuration of the form $S_\ell^x = 0$, $S_\ell^y = \sin\theta_\ell$, $S_\ell^z = \cos\theta_\ell$ where the magnitude of the classical spin has been normalized to unity. The mathematical problem then reduces to the minimization of the effective potential

$$V = \sum_{\ell=1}^{\Lambda-1} (\sin\theta_\ell \sin\theta_{\ell+1} + \Delta \cos\theta_\ell \cos\theta_{\ell+1}) - H \sum_{\ell=1}^{\Lambda} \cos\theta_\ell \tag{2}$$

0305-4470/99/183275+07$19.50

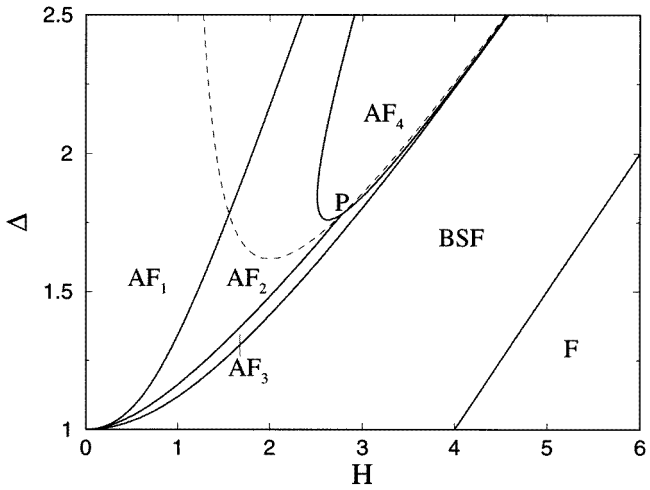

Figure 1. The classical phase diagram for an open chain and $\Delta > 1$.

where the relevant exchange constants were chosen according to $J_2 = 1$ and $J_3 \equiv \Delta > 1$. We shall further assume that the total number of lattice sites is even ($\Lambda = 2N$) and defer any comment on the case of an odd chain for a later stage of our discussion.

The minimization of V can be carried out analytically on a cyclic or infinite chain and yields three magnetic phases separated by the two critical fields

$$H_3 = 2\sqrt{\Delta^2 - 1} \qquad H_4 = 2(\Delta + 1). \tag{3}$$

For $H < H_3$ the minimum is achieved by the usual Néel states $(\theta_\ell) = (0, \pi, 0, \pi, \ldots, 0, \pi)$ or $(\pi, 0, \pi, 0, \ldots, \pi, 0)$. A bulk spin–flop (BSF) transition takes place at H_3 and the ground state becomes a canted state $\theta_\ell = (-1)^\ell \theta_0$, with $\cos\theta_0 = H/2(\Delta+1)$, in the region $H_3 < H < H_4$. Finally, the system orders ferromagnetically ($\theta_\ell = 0$) above the critical field H_4. The corresponding three phases are labelled as antiferromagnetic (AF), BSF and ferromagnetic (F) in the phase diagram of figure 1. Actually, this phase diagram also displays a rather involved fine structure in the AF phase which emerges in the presence of open boundaries and is the subject of our subsequent discussions.

Indeed, examination of local fluctuations of the Néel state on an open chain reveals the formation of surface magnon modes of the type originally discussed in the case of single-ion anisotropy by Mills and Saslow [5] and more recently in [13]. A similar analysis in the present model on a semi-infinite chain leads to a new critical field

$$H_1 = \frac{1}{2\Delta}\left[\sqrt{(\Delta^2 - 1)(9\Delta^2 - 1)} - (\Delta^2 - 1)\right] < H_3 \tag{4}$$

at which a surface magnon mode turns soft and hence the Néel state is rendered locally unstable for $H > H_1$. As a consequence, the pure AF phase shrinks down to AF_1 which corresponds to the region $H < H_1$ in figure 1. It is also worth noting that the ratio H_3/H_1 approaches the value $\sqrt{2}$ in the isotropic limit $\Delta \to 1^+$; namely, the same value as in the case of vanishing single-ion anisotropy [4–6]. When $\Delta \to \infty$ the ratio H_3/H_1 becomes equal to two, a value that may also be inferred from an elementary analysis of the extreme Ising limit.

In the region $H > H_1$ the ground state is highly nontrivial and cannot be obtained analytically on an open chain. Instead we adopt a numerical method based on a straightforward relaxation algorithm [13]. We first consider the relatively weak anisotropy $\Delta = 1.125$ for

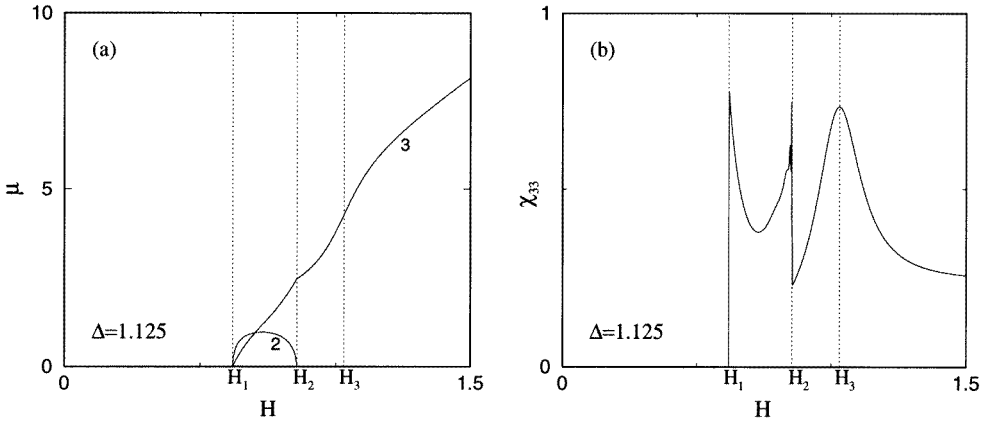

Figure 2. Field dependence of the total magnetization and susceptibility for an open chain with $\Lambda = 22$ sites and $\Delta = 1.125$. (*a*) The two nonvanishing components of the magnetization μ_2 and μ_3. (*b*) The diagonal susceptibility χ_{33} defined as in equation (5).

which the critical fields are calculated from equations (3) and (4) to be $H_1 = 0.620\,81$, $H_3 = 1.030\,78$ and $H_4 = 4.25$. The length of the chain is set at $\Lambda = 22$ which is a popular size for currently synthesized Fe/Cr superlattices [1–3]. Our numerical calculation provided detailed information on the ground-state spin configuration $S_\ell = (0, \sin\theta_\ell, \cos\theta_\ell)$, as well as on the total magnetization μ and susceptibility χ defined as

$$\mu = \sum_{\ell=1}^{\Lambda} S_\ell \equiv (\mu_1 = 0, \mu_2, \mu_3) \qquad \chi_{23} = \frac{1}{\Lambda}\frac{\partial \mu_2}{\partial H} \qquad \chi_{33} = \frac{1}{\Lambda}\frac{\partial \mu_3}{\partial H} \tag{5}$$

and illustrated in figure 2. The phase transition observed at H_1 is smoother than the one encountered in the single-ion model and may be called a first-order transition of the 'moderate type'.

Specifically, the energy is minimized by a surface state that emanates *gradually* from the Néel state as the bias field H crosses the critical value H_1. As a result, it is the susceptibility and not the magnetization that suffers a sudden jump at H_1. With further increase of the bias field beyond H_1, a new structure emerges at yet another 'critical' value:

$$H_2 = \frac{1}{2\Delta}\left[\sqrt{(\Delta^2 - 1)(9\Delta^2 - 1)} + (\Delta^2 - 1)\right] \qquad H_1 < H_2 < H_3 \tag{6}$$

or $H_2 = 0.856\,42$ for $\Delta = 1.125$. Whereas the detailed argument leading to equation (6) will not be presented in this short paper, the physical significance of the critical field H_2 should become evident from the ensuing discussion.

At sufficiently weak anisotropy the region $H_1 < H < H_2$ may be called the SSF phase, because the calculated ground-state configuration is a bona fide surface state formed near one of the two endpoints of the finite chain, and corresponds to the lower part of phase AF_2 in figure 1. As the bias field approaches H_2 the surface state organizes itself into an AF domain wall. Once nucleated, the domain wall begins to move toward the centre of the chain, with increasing bias field, and does so rapidly when H crosses H_2. The wall eventually migrates and becomes symmetric about the centre to great numerical precision near the critical field H_3; i.e., near the boundary of the anticipated BSF transition. Therefore the region $H_2 < H < H_3$ may be called the domain-wall phase and is labelled as phase AF_3 in figure 1. In fact, the BSF

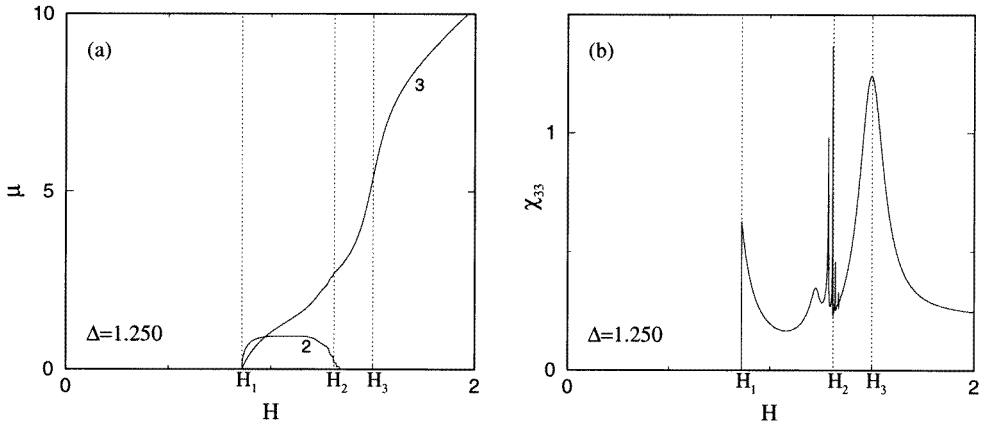

Figure 3. As figure 2 but for a stronger anisotropy, $\Delta = 1.250$.

transition is not sharp on a finite chain but is characterized by a rapid crossover behaviour when $H \sim H_3$. In the region $H \gtrsim H_3$ the domain wall expands symmetrically about the centre to become a nearly uniform canted state within the bulk with notable nonuniformities near the edges. Finally, complete F order is achieved when H crosses the last critical field H_4.

The preceding description of the ground state is clearly reflected in the field dependence of the magnetization and the susceptibility shown in figure 2. Thus, the third component of the magnetization (μ_3) gradually acquires nonvanishing values above the critical field H_1 and develops a knee at H_2. A rapid variation of μ_3 is observed near the critical field H_3, which is the finite-chain analogue of a sharp BSF transition. Beyond H_3, μ_3 increases monotonically until it reaches ferromagnetic saturation ($\mu_3 = \Lambda = 22$) at the critical field H_4 not shown in the figure range. The variation of μ_3 is more clearly demonstrated through its field derivative in figure 2(*b*). Returning to figure 2(*a*), we note that the magnetization develops a nonvanishing component also along the second direction (μ_2), mainly in the interval $[H_1, H_2]$, and hence the spin configuration is significantly twisted within the SSF phase.

Therefore, the emerging picture shares several common features with the one derived within the single-ion model [10]. But there also exist some important differences. In particular, the boundary of local stability of the Néel state ($H = H_1$) no longer coincides with the critical field H_2 where the nucleated domain wall begins to quickly move away from the surface ($H_1 \neq H_2$). The accidental coincidence of these two critical fields in the single-ion model leads to a more involved picture, especially in connection with hysteresis [12, 13], and was partly responsible for some confusion generated on that subject.

Our next concern is to examine how the derived picture evolves with increasing anisotropy. A first hint is obtained by repeating the calculation for $\Delta = 1.250$. The results for the magnetization and susceptibility are shown in figure 3 and display a great deal of fine structure around the critical field H_2. This structure suggests a complicated energy landscape of the effective potential (2) analogous to that occurring in the single-ion model [7–9]. The picture becomes increasingly involved for intermediate anisotropies in the neighbourhood of $\Delta \sim 2$.

In order to temporarily sidestep the complexities of the intermediate regime, we consider the case of strong anisotropy where the picture is again simplified. A surface state is still formed when the bias field crosses H_1 and persists over a nontrivial region above H_1 until it regroups itself into a domain wall. The main difference from the weak-anisotropy region is that the nucleated domain wall is now an ideal Ising wall located right at the boundary of

the chain; namely, $(\theta_\ell) = (0, 0, \pi, 0, \pi, 0, \ldots) \equiv |0\rangle$. Here we adopt [10] the convenient symbol $|2n\rangle$, with $n = 0, 1, 2, \ldots$, to denote an Ising domain wall located n steps away for the chain boundary; e.g. $|2\rangle = (0, \pi, 0, 0, \pi, 0, \ldots)$, and so on. An ideal Ising wall is an exact *stationary* point of the effective potential and, once created, will persist as the relevant ground-state configuration for all field values H for which it is *locally stable* at a given anisotropy Δ. Examination of quadratic fluctuations around the stationary point $|0\rangle$ yields an algebraic condition that determines the boundary of its local stability, namely

$$2\Delta H^4 - 2(4\Delta^2 - 1)H^3 + 5\Delta(2\Delta^2 - 1)H^2 - (4\Delta^4 - 5\Delta^2 + 1)H - 2\Delta(\Delta^2 - 1) = 0. \quad (7)$$

The roots of this equation in the upper-right quadrant of the (Δ, H) plane were obtained numerically and provided the boundary of phase AF_4 in figure 1.

Within AF_4 the Ising domain wall $|0\rangle$ is locally stable and is the relevant ground-state configuration when the bias field is increased adiabatically, either continuously or in small steps. Putting it differently, the state $|0\rangle$ persists even when it eventually becomes metastable in the sense that its energy becomes higher than the energy of other local minima of the effective potential. However, when the field exceeds the right boundary of the AF_4 phase, one enters again the domain-wall phase AF_3 in which the Ising wall $|0\rangle$ initially spreads out to some extent and then quickly migrates to the centre of the chain; in analogy with the picture described earlier for weak anisotropy. A byproduct of this analysis is that the critical boundary H_2 of equation (6) is not meaningful at strong anisotropy and is thus terminated at the 'multicritical point' P, in figure 1, which is defined as the intersection of $H = H_2(\Delta)$ and the boundary of the AF_4 phase calculated from equation (7). Explicitly one finds that $P = (\Delta, H) = (1.780\,7764, 2.780\,7764)$.

The multicritical point is endowed with the following remarkable property. The boundaries of local stability of the Ising domain walls $|2n\rangle$, denoted by $H_{[2n]} = H_{[2n]}(\Delta)$ with $n = 0, 1, \ldots, \infty$, all intersect at the point P calculated in the preceding paragraph. The special case $H_{[0]}$ is the boundary of the AF_4 phase calculated from equation (7), while the other extreme member of the family is given by

$$H_{[\infty]} = \frac{2}{2\Delta + 1}\left[\Delta(\Delta + 1) \pm \sqrt{\Delta(\Delta + 1)(\Delta^2 - \Delta - 1)}\right]. \quad (8)$$

The corresponding curve is shown by a dashed curve in figure 1 and provides the lower boundary of the region of local stability of an ideal Ising wall located well within the bulk of the chain. Outside that region the wall stabilizes by spreading out to become a topological defect with a nontrivial spatial distribution. A notable fact is that an ideal Ising wall is unstable at vanishing field for any finite value of Δ, however large; in contrast to the situation in the single-ion model where Ising walls can be stable even at vanishing field provided that the anisotropy exceeds a certain critical value [10, 17].

The preceding results should prove helpful for a more detailed understanding of the intermediate regime but we shall not pursue such an analysis further in this paper. We thus conclude our discussion of the classical XYZ model with two brief comments.

First, we note that all analytical results leading to the phase boundaries of figure 1 were derived on a semi-infinite chain, whereas the numerical results of figures 2 and 3 were obtained on a finite chain with $\Lambda = 22$ sites. However, the AF_1: AF_2 boundary predicted analytically by equation (4) agrees with the numerically calculated boundary at $\Lambda = 22$ and $\Delta = 1.125$ to eight significant figures, while greater accuracy is achieved for longer chains or stronger anisotropy. Deviations from the analytical predictions may emerge in the extreme isotropic limit $\Delta \to 1^+$ which requires a numerical calculation on increasingly longer chains. Similarly, the bulk spin–flop transition anticipated to occur at the AF_3: BSF boundary is actually replaced by a rounded crossover transition on a finite chain, which becomes sharp as the chain size increases.

Secondly, we comment on the case of an odd chain ($\Lambda = 2N+1$). The main difference in the Néel state of an odd chain is that the two outer spins point in the same direction. Therefore when the bias field is applied along the common direction of the outer spins a SSF transition is absent and the chain proceeds directly to the BSF transition. When the field is applied in the opposite direction a SSF transition takes place at both ends. Hence the study of an odd open chain does not appear to add anything fundamentally new.

While the classical analysis reveals a rich phase diagram due to surface effects, the situation is less clear for quantum spin chains. An important special case is the spin $-\frac{1}{2}$ Heisenberg–Ising chain ($J_1 = 1 = J_2$, $J_3 = \Delta > 1$) immersed in a bias field H pointing along the symmetry axis. The Hamiltonian may then be diagonalized through the Bethe ansatz [14] and the effect of the bias field is simply a linear Zeeman shift of the zero-field eigenvalues. Accordingly the question of spin–flop transitions becomes a problem on level crossings induced by the applied field. The $T = 0$ phase diagram on a cyclic or infinite chain was already considered by Johnson and McCoy [18] and consists of three magnetic phases, for $\Delta > 1$, corresponding to the bulk AF, BSF and F classical phases of figure 1. Equivalently, the calculation of [18] furnished the quantum analogues of the critical fields H_3 and H_4 of equation (3). The F boundary H_4 is the same in the classical and quantum cases, as expected, but the quantum analogue of H_3 is significantly different and vanishes exponentially in the isotropic limit $\Delta \to 1^+$.

The remaining important question is then to determine whether or not the phase diagram of [18] acquires fine structure due to surface effects analogous to that displayed in our classical phase diagram of figure 1. An elementary consideration of magnon excitation gaps in the extreme Ising limit ($\Delta \to \infty$) does indeed suggest the existence of a critical field H_1 such that $H_3/H_1 = 2$ which is, of course, the same ratio as the one obtained in the classical calculation. Therefore the immediate question is to follow the above observation down to finite anisotropy Δ and eventually calculate the ratio H_3/H_1 in the limit $\Delta \to 1^+$ where the classical model suggests the value $\sqrt{2}$. Of course, the classical model is valid for large spin s and its detailed predictions may not be reliable at $s = \frac{1}{2}$. However, as is often the case, the broad features of the classical calculation may survive in the quantum theory, at least for some nontrivial parameter region in the range $|J_1| \leqslant J_2$. Although there have been a large number of recent investigations of the quantum model addressing surface effects in the presence of (local) boundary fields [19, 20], the straightforward question posed here in the absence of such fields does not seem to have been answered.

References

[1] Wang R W, Mills D L, Fullerton E E, Mattson J E and Bader S D 1994 *Phys. Rev. Lett.* **72** 920
[2] Wang R W, Mills D L, Fullerton E E, Kumar S and Grimsditch M 1996 *Phys. Rev.* B **53** 2627
[3] Rakhmanova S, Mills D L and Fullerton E E 1998 *Phys. Rev.* B **57** 476
[4] Mills D L 1968 *Phys. Rev. Lett.* **20** 18
[5] Mills D L and Saslow W 1968 *Phys. Rev.* **171** 488
[6] Keffer F and Chow H 1973 *Phys. Rev. Lett.* **31** 1061
[7] Trallori L, Politi P, Rettori A, Pini M G and Villain J 1994 *Phys. Rev. Lett.* **72** 1925
[8] Trallori L, Politi P, Rettori A, Pini M G and Villain J 1995 *J. Phys.: Condens. Matter* **7** L451
[9] Trallori L 1998 *Phys. Rev.* B **57** 5923
[10] Micheletti C, Griffiths R B and Yeomans J M 1997 *J. Phys. A: Math. Gen.* **30** L233
[11] Micheletti C, Griffiths R B and Yeomans J M 1999 *Phys. Rev.* B in press
[12] Papanicolaou N 1998 *J. Phys.: Condens. Matter* **10** L131
[13] Papanicolaou N 1999 *J. Phys.: Condens. Matter* **11** 59
[14] Gaudin M 1983 *La Fonction d'Onde de Bethe* (Paris: Masson)
[15] Asakawa H, Matsuda M, Minami K, Yamazaki H and Katsumata K 1998 *Phys. Rev.* B **57** 8285
[16] Gelfand M P and Glöggler E F 1997 *Phys. Rev.* B **55** 11 372

[17] Papanicolaou N 1995 *Phys. Rev.* B **51** 15 062
[18] Johnson J D and McCoy B M 1972 *Phys. Rev.* A **6** 1613
[19] Jimbo M, Kedem R, Kojima T, Konno H and Miwa T 1995 *Nucl. Phys.* B **441** 437
[20] Kapustin A and Skorik S 1996 *J. Phys. A: Math. Gen.* **29** 1629